

## Accepted Manuscript

A liquid foam-bed photobioreactor for microalgae production

Agnes Janoska, Packo P. Lamers, Alex Hamhuis, Yorick van Eimeren, Rene H. Wijffels, Marcel Janssen

PII: S1385-8947(16)31584-4  
DOI: <http://dx.doi.org/10.1016/j.cej.2016.11.022>  
Reference: CEJ 16023

To appear in: *Chemical Engineering Journal*

Received Date: 16 August 2016  
Revised Date: 21 October 2016  
Accepted Date: 4 November 2016

Please cite this article as: A. Janoska, P.P. Lamers, A. Hamhuis, Y. van Eimeren, R.H. Wijffels, M. Janssen, A liquid foam-bed photobioreactor for microalgae production, *Chemical Engineering Journal* (2016), doi: <http://dx.doi.org/10.1016/j.cej.2016.11.022>

This is a PDF file of an unedited manuscript that has been accepted for publication. As a service to our customers we are providing this early version of the manuscript. The manuscript will undergo copyediting, typesetting, and review of the resulting proof before it is published in its final form. Please note that during the production process errors may be discovered which could affect the content, and all legal disclaimers that apply to the journal pertain.



## A liquid foam-bed photobioreactor for microalgae production

**Agnes Janoska\*<sup>a</sup>, Packo P. Lamers<sup>a</sup>, Alex Hamhuis<sup>a</sup>, Yorick van Eimeren<sup>a</sup>, Rene H.**

**Wijffels<sup>a, b</sup>, Marcel Janssen<sup>a</sup>**

<sup>a</sup> AlgaePARC, Bioprocess Engineering, Wageningen University and Research, P.O. Box 16, 6700AA, Wageningen, The Netherlands. Internet: [www.wageningenur.nl/bpe](http://www.wageningenur.nl/bpe), [www.algaeparc.com](http://www.algaeparc.com) and [www.miraclesproject.eu](http://www.miraclesproject.eu)

<sup>b</sup> Faculty of Biosciences and Aquaculture, Nord University, N-8049, Bodø, Norway

\*Corresponding author: Agnes Janoska

Email addresses:

Agnes Janoska      [agnes2.janoska@wur.nl](mailto:agnes2.janoska@wur.nl)

Marcel Janssen      [marcel.janssen@wur.nl](mailto:marcel.janssen@wur.nl)

## Highlights

- Proof of principle of a foam-bed photobioreactor for microalgae cultivation.
- A method for continuous foam breaking was established.
- *Chlorella* cultures survive shear stress linked to bubble formation and burst.
- A growth rate of  $0.1 \text{ h}^{-1}$  was achieved for *Chlorella sorokiniana*.

## Abstract

A novel concept of cultivating microalgae in liquid foam was developed with the intention of reducing biomass production costs. This cost reduction is based on reduced harvesting costs due to high biomass densities, and reduced energy requirements due to improved mass transfer and lower pressure drop in the foam-bed photobioreactor. Foam generation could be controlled by adding foaming agents and employing homogenous gas distribution at the bottom of the photobioreactor. In order to refresh the gas phase entrapped in the bubbles, and ensure sufficient  $\text{CO}_2$  for microalgal growth, different foam break-up methods were evaluated. A packed bed filled with large hydrophobic beads resulted in efficient foam break-up at minimal pressure drop. It was shown that microalgae (*Chlorella sorokiniana*) can grow in the liquid channels of liquid foams stabilised by the protein Bovine Serum Albumin, and that the culture can withstand the physical processes of foam formation and foam break-up. An average growth rate of  $0.10 \text{ h}^{-1}$  was observed. The quantum yield of photosystem II photochemistry remained maximal during the reactor runs, indicating that photosynthesis was not impaired. The results obtained show that cultivation of microalgae in liquid foams is a promising new concept.

**Keywords:** Microalgae cultivation; Photobioreactor; Foam-bed reactor; Liquid-foam

## 1. Introduction

The production of useful substances of algal origin, including specialities for food and aquaculture as well as biofuels and bulk chemicals, requires energy-efficient and economically profitable cultivation systems [1-3]. Many studies highlighted the importance of photobioreactor design and operation as major factors influencing production costs [4-7]. The goal of this study is therefore the development of a novel microalgae cultivation system that could enable economically feasible microalgae cultivation by reducing biomass production costs. The major factors that determine the practical application of photobioreactors is rapid and energy-efficient transfer of carbon dioxide and oxygen [8], the dewatering of the harvested, dilute microalgal cultures [9], and the high energy input for aeration [10]. In this study a foam-bed photobioreactor with high gas holdup was developed since increased gas holdup results in both increased mass transfer and lower pressure drop. In addition, the foam-bed photobioreactor supports increased biomass concentration due to the thin liquid layers between the foam bubbles reducing microalgal self-shading. The concept of growing microalgae in liquid foam-bed photobioreactors is an innovative idea in the field of microalgae cultivation [11].

In a foam-bed reactor small gas bubbles are passed through a thin liquid layer resulting in foam generation. The liquid is either self-foaming or contains a foam stabilising agent. Thus, the culture is composed of a thin liquid layer at the bottom of the reactor with a large volume of foam exposed to (sun)light, above it. Due to the continuous gas supply, the generated foam bubbles rise. Simultaneously, the liquid film separating adjacent gas bubbles is continuously draining downwards due to gravity.

This novel concept has several potential advantages over traditional cultivation systems. First, when adopting flat-panel photobioreactors in combination with a liquid foam-bed the light path in the liquid film in the foam over which light absorption takes place is in the order of a few millimetres only. Consequently, the biomass concentration can be increased with an order of magnitude ( $\geq 10 \text{ g L}^{-1}$ ) compared to liquid-filled flat-panel reactors, thereby reducing downstream processing costs with the same factor. Furthermore, a foam-bed reactor only contains a limited water volume (about 5% v/v) resulting in a low pressure drop relative to the height of the photobioreactors. Therefore, the concept might enable energy reduction on gassing due to the low pressure drop present in the reactor. Besides, due to the low pressure drop in the reactor, the carrier capacity of the structure supporting the photobioreactors can be reduced considerably, thereby lowering construction costs of large-scale systems. Also, the high interfacial area created between the gas and water with microalgae contributes to the reduced energy requirement of the foam-bed reactor. The high interfacial area results in a high transfer capacity for both oxygen and carbon dioxide. Finally, the residence time of the gas in the photobioreactor is increased by orders of magnitude since the gas is entrained within the liquid films of the foam. This leads to a much more efficient use of carbon dioxide.

Foam-bed reactors for chemical-physical treatment of gases are known. Owing to the enhanced mass transfer capacity and low pressure drop of these systems, efficient contaminant removal of gas streams is possible. In these reactor systems, components of the gas move from the gas bubbles to the thin liquid films, followed by a chemical reaction in the liquid phase of the foam [12-14]. Foam-bed reactors are also used as bioreactors for contaminant removal from gas streams [15-20]. In these systems the pollutant-degrading microorganisms are grown in the thin liquid films in the foams. The performance of foamed emulsion bioreactors (a type of foam-bed bioreactor, where organic phase emulsion and

pollutant-degrading microorganisms are foamed and the resulting gas bubbles contain the pollutant) exceed the performance of any other reactor system for air pollutant control [16]. These reactors rely on high density cultivation of microorganisms in order to reach high removal rates, increased gas-liquid interfacial area provided by the foams, and elimination of clogging problems compared to immobilized beds [16].

For the design of a foam-bed reactor, foam formation and foam break-up are fundamental. The properties of the formed foams are dependent on the gas distributor design, as it influences the bubble size of the foam. More specifically, if the gas distributor creates smaller bubbles, more stable and wet foam will be formed [21]. In contrast, larger bubbles will rise faster to the surface and collapse more rapidly [22]. Besides gas distribution, also the gas flow rate and surfactant concentrations play key roles in determining the foam properties.

In order to support maximal microalgae production in a foam-bed photobioreactor, the CO<sub>2</sub> supply must be sufficient. For this reason, the foam bubbles have to be broken in order to refresh the entrapped gas. Ideally, a foam bubble ruptures just before the carbon dioxide is depleted, and/or oxygen builds up to inhibiting levels. For inducing foam break-up, various methods have been reported in literature. The simplest method is spontaneous, self-break-up of the foam [18]. This method is based on natural destabilisation mechanisms, including foam drainage, coalescence, and coarsening. Liquid drainage from the foam is caused by gravity and causes thinning of the liquid films between bubbles. This thinning can lead to film rupture, resulting in coalescence of the neighbouring bubbles. Coarsening takes place due to gas diffusion from the small bubbles to the larger ones, due to the pressure difference inside them. All these processes can result in bubble growth and eventually to foam destabilisation [23].

Another, commonly used method is the use of chemical antifoams or defoamers [12, 24-27]. These methods are efficient in destroying and controlling foams, but in several cases they cannot be used. For instance, the antifoaming agents can adsorb to cell surfaces and consequently inhibit growth of the microorganism, they can cause contamination, reduce mass transfer, and exhibit adverse effect on downstream processing of the product (e.g. separation, purification) [28-30]. Foam breaking by mechanical means is free of such problems, however, substantial power is required for the operation of the devices [30]. Mechanical methods are mainly based on shear forces [28], or on centrifugal forces [31], and they include spraying liquid on the foam [16, 20, 32] or breaking the foam by rotating parts [21, 29, 33]. Mechanical and ultrasonic vibrations are also often used [28]. Compared to chemical or mechanical foam breaking methods, a foam eliminating net [34] can reduce the operational costs and the contamination of the media can be prevented. Together, these studies highlight the variety of possibilities for foam break-up, which is a crucial factors in establishing and further improving foam-bed reactor systems.

This study aims to develop a liquid foam-bed photobioreactor for microalgal growth with continuous foam formation and foam break-up. For that, optimal foam formation settings were experimentally defined and also an efficient foam break-up method was developed. Furthermore, the possibility of microalgal growth in protein stabilised foams was evaluated. In order to assess whether microalgae are able to withstand the shear stresses involved in foam formation and break-up, the biomass concentration and the quantum yield of photosystem II photosystem were monitored.

## 2. Materials and Methods

### 2.1 Experimental set-up

The experimental set-up consisted of a foam-bed photobioreactor, a foam breaker column and a recirculation pump (Figure 1). The foam-bed photobioreactor itself consisted of a flat panel reactor chamber and an adjacent water chamber for temperature control. The reactor had a height of 40 cm, and a width of 20 cm. The reactor had a depth of 2.7 cm and the reactor volume was approximately 2.2 L. The reactor had round edges on the top in order to avoid foam to accumulate and remain there. The reactor plates were made of glass and the reactor frame was made of polyether ether ketone (PEEK). The glass plates were treated with a solution of concentrated sulfuric acid (98 wt.%) and hydrogen peroxide solution (30 wt.%) in a 3:1 ratio. This solution cleaned the glass surface and rendered it hydrophilic; a contact angle of  $12^\circ$  was reported [35]. The cleaned glass plates were washed with distilled water. The contact of the foam with hydrophilic walls, as opposed to hydrophobic surfaces, had a positive effect on foam stability inside the reactor, enabling faster foam rise and reducing the extent of coalescence at the walls.

The inlet gas was composed of 5.5 v/v % carbon dioxide in nitrogen gas and was supplied with a total flow rate of  $614 \text{ NmL min}^{-1}$  by mass flow controllers (Brooks Instrument B.V. Model 5850S). This gas was filtered with  $0.2 \mu\text{m}$  filters (Whatman Polyvent 500) prior to entering the reactor. The filtered gas was distributed through a stainless steel gas distributor with small conical holes ( $30 \mu\text{m}$  and  $100 \mu\text{m}$  hole diameter on the top and the bottom of the cone, respectively). The gas distributing plate was placed on the bottom of the reactor, enabling bubble formation over 40% of the cross sectional area in order to ensure good mixing and avoid microalgae settling. The gas distributor created a large number of small, homogenous bubbles stimulating continuous foam formation. The foam rising to the top of



the reactor was allowed to leave through three outlets (0.9 cm diameter) and was led to the foam breaker device via silicone tubing with 0.8 cm diameter. These three separate outlets (2 at the sides and one in the middle) were required in order to avoid foam to accumulate and remain in the reactor.

As a foam breaker device, a packed bed column filled with hydrophobic beads was established. The internal diameter of the glass column was 5 cm and it had a volume of 216 mL. The glass surface was rendered hydrophobic by applying a coating called Sigmacote (Sigma-Aldrich). The hydrophobic beads had an average diameter of 6.3 mm and were made of polytetrafluoroethylene (PTFE) produced by FTL Technology, and they were mixed with polydimethylsiloxane (PDMS) cubes of approximately the same size. The PDMS cubes were fabricated from a Silicone Elastomer Kit (Sylgard 184 Silicone Elastomer and curing agent, Dow Corning) and the ratio of the base monomers and the curing agent was 10:1. After mixing and eliminating the gas bubbles, the mix was poured in a glass petri dish. The PDMS was cured for 1 hour in the oven at 80°C. After cooling overnight, the PDMS sheet was removed from the petri dishes and placed in the oven at 60°C for overnight. This PDMS slab was afterwards cut to small pieces with a sharp knife.

After the foam entered from the top into the foam breaker, it was led through the packed bed column and subsequently ended up in a vessel for gas-liquid separation, as depicted in Figure 1. The liquid was pumped back to the reactor by a peristaltic pump. The liquid volume in the photobioreactor was controlled by avoiding evaporation or condensation inside the reactor.

The nitrogen gas was humidified by leading it through a 4 mm inner diameter tubing to the bottom of a 500 mL water bottle kept at 2°C. Dry CO<sub>2</sub> gas was mixed with the humidified N<sub>2</sub>

gas before entering the reactor. The gas left the reactor through a condenser maintained at 2°C.

A pH and temperature sensor were incorporated in the reactor. The temperature sensor was placed at the top of the reactor, measuring the temperature of the upper third part of the foam. The pH was measured within the foam-bed at the bottom just above the bulk liquid level. The pH was not controlled but it remained  $6.7 \pm 0.3$  throughout the experiments. The culture temperature was maintained at 37°C by controlling the temperature in the water jacket by recirculating the water through a water bath. The reactor was illuminated from one side by two warm-white LED floodlights with a 45 mil Bridgelux LED chip, stacked on top of each other providing an intensity of  $334 \pm 16 \mu\text{mol PAR photons m}^{-2} \text{s}^{-1}$  across the reactor surface. Pictures of the foam-bed photobioreactor are presented in Figure 2.

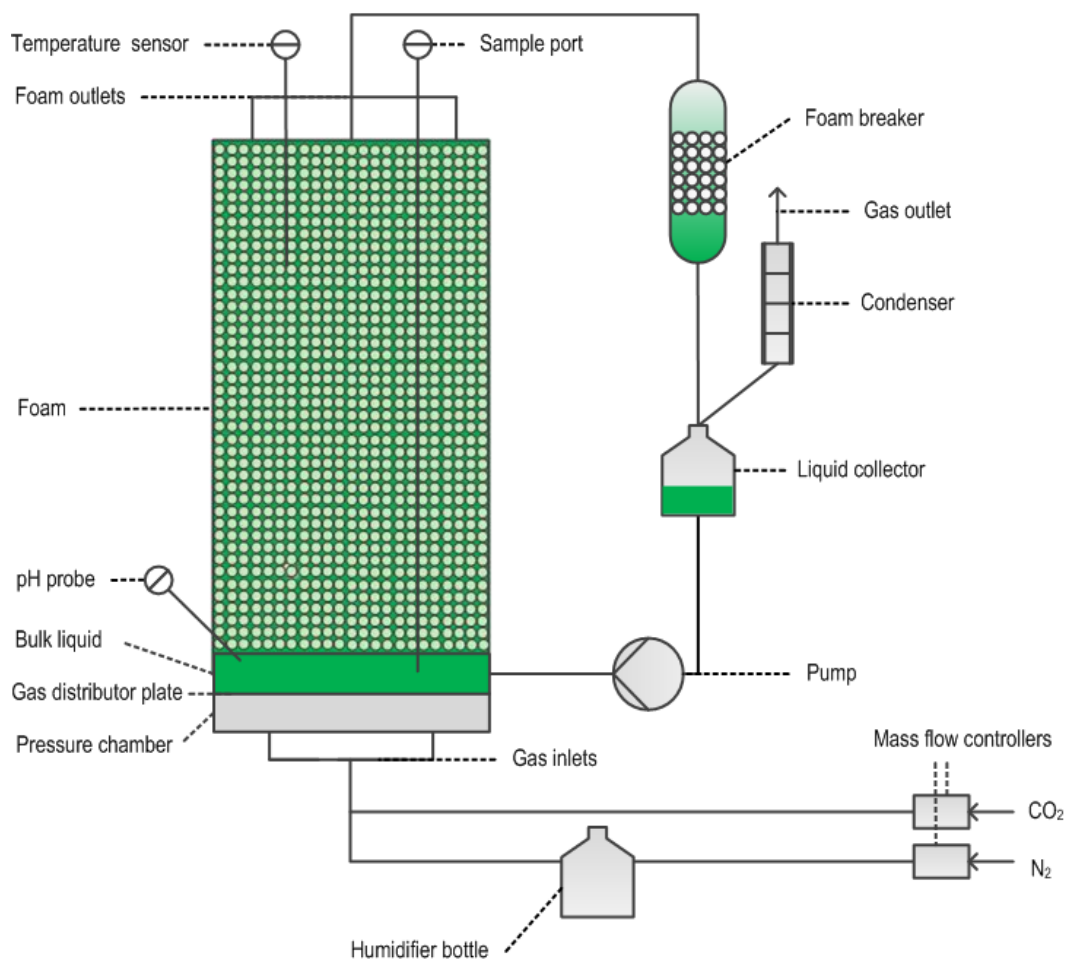


Figure 1: Schematic overview of the foam-bed photobioreactor. Gas is fed at the bottom of the reactor via a gas distributor plate, releasing fine gas bubbles into the bulk liquid, continuously creating foam. The foam leaves the reactor on the top and is then transported towards the foam breaker. After break-up of the foam the separated liquid and gas phase end up in a collector vessel from where the gas leaves through the condenser and the liquid is pumped back into the reactor.

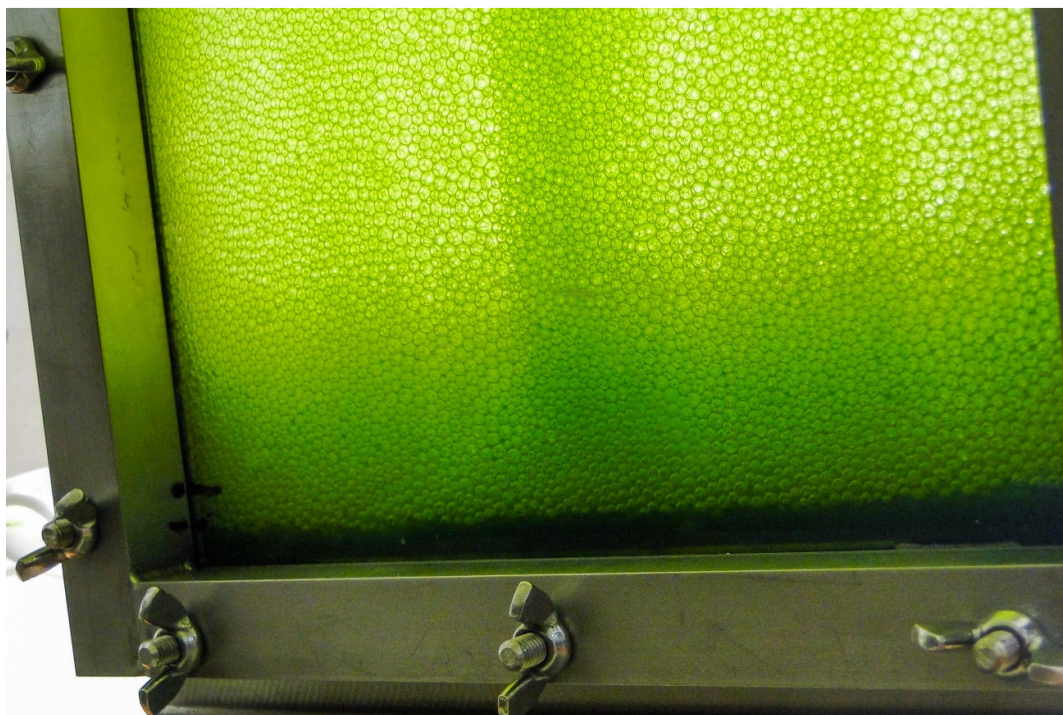


Figure 2: Picture of the foam in the foam-bed reactor containing microalgae.

## 2.2 Microalga and growth medium

*Chlorella sorokiniana* strain CCAP 221/8K was obtained from the Culture Collection of Algae and Protozoa (CCAP, Oban, Scotland). *C. sorokiniana* was grown in shake flasks, on a media based on 3 times concentrated M8a media [36], containing the following nutrients: urea 60 mM,  $\text{KH}_2\text{PO}_4$  7.88 mM,  $\text{Na}_2\text{HPO}_4 \cdot 2\text{H}_2\text{O}$  2.12 mM,  $\text{MgSO}_4 \cdot 7\text{H}_2\text{O}$  4.87 mM,  $\text{CaCl}_2 \cdot 2\text{H}_2\text{O}$  0.26 mM, EDTA ferric sodium salt 948  $\mu\text{M}$ ,  $\text{Na}_2\text{EDTA} \cdot 2\text{H}_2\text{O}$  300  $\mu\text{M}$ ,  $\text{H}_3\text{BO}_3$  3  $\mu\text{M}$ ,  $\text{MnCl}_2 \cdot 4\text{H}_2\text{O}$  196.76  $\mu\text{M}$ ,  $\text{ZnSO}_4 \cdot 7\text{H}_2\text{O}$  33.39  $\mu\text{M}$ ,  $\text{CuSO}_4 \cdot 5\text{H}_2\text{O}$  21.99  $\mu\text{M}$ . After the addition of all nutrients, the pH was adjusted with NaOH to pH 6.7. The same medium supplemented with 5 mM  $\text{NaHCO}_3$ , (after setting of the pH), was used for both the pre-cultivation and the foam-bed photobioreactor experiments.

The inoculum for the foam-bed photobioreactor was pre-grown in an airlift flat-panel photobioreactor, as described by de Mooij et al. [37]. This reactor was operated continuously

with a dilution rate of  $0.106 \text{ h}^{-1}$ . The pH was controlled at 6.7 by  $\text{CO}_2$  addition. The incident light intensity was  $1400 \mu\text{mol photons m}^{-2} \text{ s}^{-1}$ . This ensured an exponentially growing algal culture acclimated to high light intensities, thereby avoiding a lag phase during growth in the foam-bed photobioreactor. To inoculate this photobioreactor, cultures cultivated in shake flasks were used. These shake flasks were kept in an incubator containing 4 %  $\text{CO}_2$ , operated at  $37^\circ\text{C}$ ,  $454 \mu\text{mol photons m}^{-2} \text{ s}^{-1}$  and 120 rpm.

### 2.3 Growth experiments foam-bed photobioreactor

Prior to the growth experiments, the reactor was autoclaved to ensure sterile operation. The reactor was started with 150 mL of culture medium containing  $1.75 \text{ g L}^{-1}$  bovine serum albumin (BSA, Sigma-Aldrich) as a protein-based foaming agent. This medium was inoculated with *Chlorella sorokiniana* cultures to an optical density (750 nm) of  $5.6 \pm 0.7$  units (equivalent to  $2.1 \pm 0.2$  gram dry biomass per litre). After starting the gas supply to the reactor, the initial liquid present separated into two different segments: the wet foam phase and the remaining liquid layer on the bottom of the reactor above the gas distributing plate, referred to as the bulk liquid. The bulk liquid area was covered with aluminium foil to shade off light in order to avoid growth in that segment. Samples (2 to 3 mL) were taken each 2 hours from the reactor bulk liquid and were analysed for algae concentration (optical density, cell number, and cell volume concentration), the maximum quantum yield of PSII photochemistry ( $F_v/F_m$ ), and the protein concentration. The temperature and pH inside the reactor were continuously monitored. The temperature and relative humidity of the outgoing gas was analysed at two hour intervals. The relative humidity of the ingoing gas was measured before the experiments using a humidity meter (HI, Testo Inc.). The water level and temperature of the humidifying bottle were kept constant, thus the initially measured humidity was representative for all the experiments.

## 2.4 Analytical methods

The microalgae concentration in the samples was determined by two different methods. Firstly, spectrophotometric analysis (DR 600 spectrophotometer from Hach Lange) was carried out. The measuring wavelengths employed were 680 nm and 750 nm. The second method used was measuring cell number and cell volume concentration with a Beckman Coulter Multisizer 3 employing a 50 $\mu$ m aperture tube. The cell size distribution was determined in terms of cell volumes, from which the total cell volume concentration was calculated.

The BSA protein concentration in solution was determined by the Lowry method. Prior to analysis, samples were centrifuged at 20,000 RCF for 10 minutes to remove algae and bacteria from the sample. Supernatants were stored at -24 °C until analysis. These samples were diluted to a protein concentration less than 1.4 g L<sup>-1</sup>. Afterwards the Bio-Rad Dc protein assay kit was used for the analysis. The absorbance was determined by a measurement at 750nm using the Tecan M200 Plate Reader, and a calibration curve made with BSA was used to convert the absorbance values to concentrations expressed in g L<sup>-1</sup>.

Maximum photosystem II quantum yield was measured based on chlorophyll fluorescence with the AquaPen-C AP-C 100 fluorimeter (PSI, Czech Republic) [38]. Samples were diluted to an optical density (OD) at 750 nm of approximately 0.1 unit. The minimal fluorescence level was measured after 15 minutes incubation in the dark at a light intensity of 0.03  $\mu$ mol photons m<sup>-2</sup> s<sup>-1</sup> at 455 nm. The maximal fluorescence was measured after a light pulse of 3000  $\mu$ mol photons m<sup>-2</sup> s<sup>-1</sup>. The maximum photosystem II quantum yield ( $F_v/F_m$ ) is calculated as the difference of the maximal fluorescence of the sample ( $F_m$ ) and the minimal fluorescence ( $F_0$ ), divided by the maximal fluorescence, resulting in  $(F_m-F_0)/F_m$ .

Properties of BSA-stabilized foam were analysed by an automated foam analyser (Foamscan, Teclis- IT Concept, Logessaigne, France), adapted from Lech et al. [39]. Firstly, foam is generated by blowing nitrogen gas through a metal frit with small conical holes (30  $\mu\text{m}$  and 100  $\mu\text{m}$  hole diameter on the top and the bottom of the cone, respectively) to a glass cylinder containing 60 mL of surfactant solution. After the foam volume has reached 400  $\text{cm}^3$ , the gas flow automatically stops. The liquid volume of the solution remaining on the bottom of the cylinder was monitored by conductimetry. The amount of liquid incorporated in the foam was calculated as the difference between the initial liquid volume and the liquid volume at the different time points. The volume percentage of liquid within the foam will be further referred to as the liquid holdup of the foam. The maximal liquid holdup represents the liquid holdup of the foam at the moment when the foam has reached its desired height and the gas distribution has been terminated. The foam volume was followed in time by a camera and consequent image analysis. Foam stability was measured in terms of the time needed until half of the foam volume had collapsed, and will be further referred to as the foam half-life ( $t_{1/2}$ ). The evolution of the bubble sizes was monitored by image analysis. Pictures were taken each 30 seconds after the gas flow had stopped, at a height of 8 cm above the gas distributor. The bubble size was calculated by image analysis software (Foamscan), from the first picture of the static foam. The temperature of the glass cylinder was kept at  $37 \pm 2$   $^{\circ}\text{C}$  in all experiments, and controlled by a water bath. The gas flow rate for the experiments with different surfactant concentrations was  $400 \text{ cm}^3 \text{ min}^{-1}$ , resulting in  $2.4 \text{ mm s}^{-1}$  superficial gas velocity. The BSA concentration for the experiments with different gas flow rates were  $0.5 \text{ g L}^{-1}$ . The experiments were performed in duplicate.

### 3. Results and Discussion

#### 3.1 System design

In this section the most important aspect of the design of the foam-bed photobioreactor are presented.

##### 3.1.1 Optimization of foam formation

In this study, Bovine Serum Albumin (BSA) was selected as foam stabilising agent. This surfactant is biocompatible [40, 41] and has a good foaming ability [42]. Firstly, the properties of foams formed by different BSA concentrations and different gas flow rates were determined. The observed relations were then applied to select optimal conditions for the operation of the foam-bed photobioreactor. This optimization aimed to create a wet and homogeneous foam in the reactor, which could be easily destabilized in the foam-breaker.

Initially, protein foams were analysed with an automated foam analyser (Foamscan). Foam stability in terms of foam volume half-life, liquid holdup of the foam, and bubble size were analysed as a function of BSA concentration and applied gas flow rates. In the range investigated, the protein concentration has more impact on bubble size, liquid holdup and foam stability compared to the gas flow rate. The results show that higher BSA concentrations result in smaller bubble sizes and more stable foams with higher liquid holdup (Figure 3 A, B, and C). These results are in agreement with other studies, and the underlying mechanism is described as follows. Increasing the surfactant concentration results in a lower surface tension, which in turn leads to a smaller bubble size, resulting in a wetter and more stable foam [21, 28]. Higher superficial gas velocities have similar effect: at increased gas velocities, slightly smaller bubbles are formed, resulting in increased foam stability and liquid holdup (Figure 3 D, E and F). At higher gas flow rates, the foam liquid holdup is increased due to the elevated upward liquid flux [43]. At low gas flow rates the time to reach a given volume is



increased, which results in increased foam destabilisation. The longer time period for foam formation contributes to the decreased liquid holdup [44] and possibly this also adds to the decreased foam stability occurring at reduced gas flow rates. A closer look on the graphs presented in Figure 3 show that a decreasing bubble size goes together with a more stable and wet foam. At increased gas flow rates and at increased surfactant concentrations the foam appeared more homogenous, as also expressed by the standard deviations of the average bubble sizes (Figure 3 C and F).

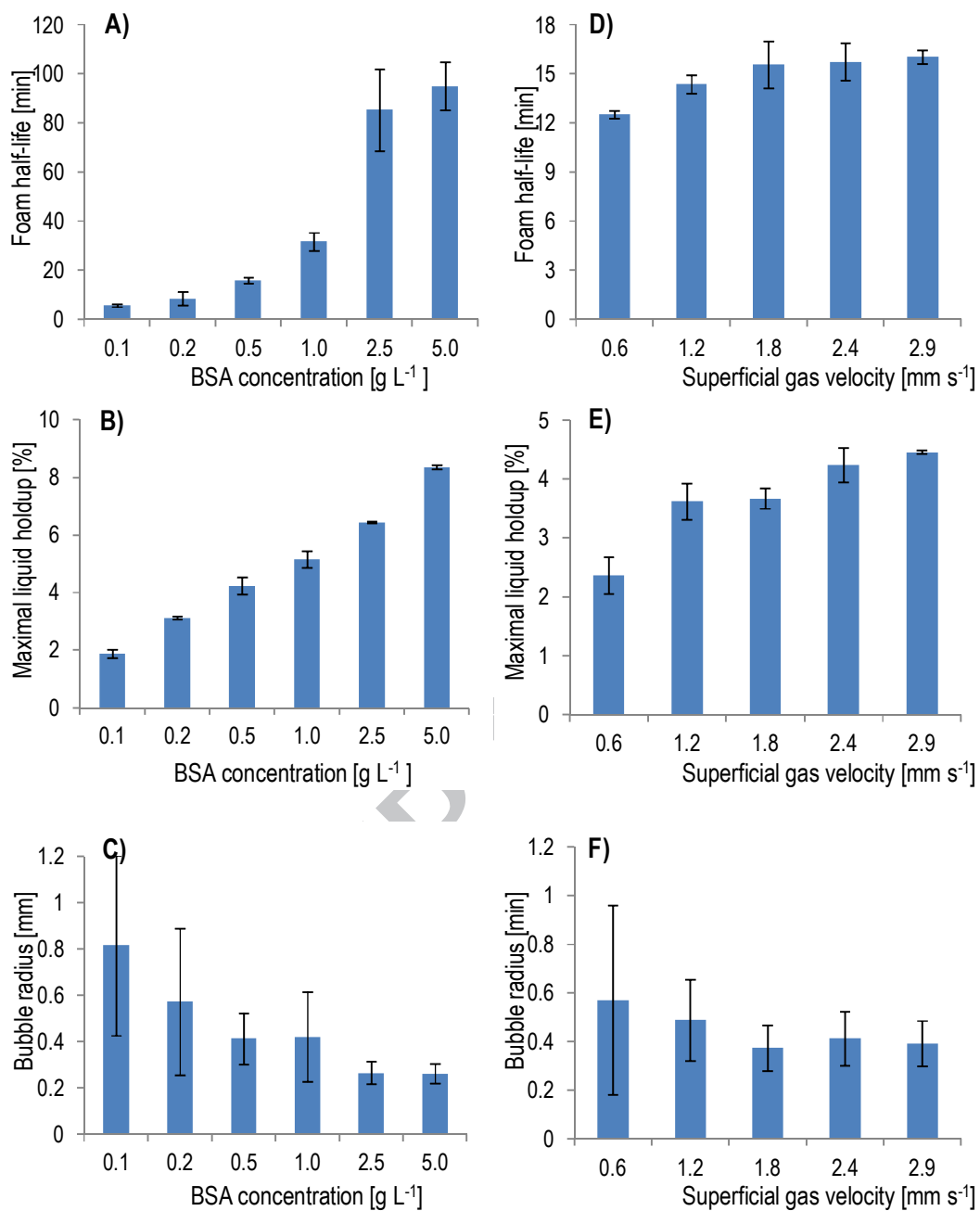


Figure 3: Effect of BSA concentration on the half-life of the foam (A), the maximal liquid holdup of the foam (B), and the average bubble radius of the foam (C). Effect of superficial gas velocity at 0.5 g L<sup>-1</sup> BSA on the half-life of the foam (D), the maximal liquid holdup of the foam (E), the average bubble radius of the foam (F).

Based on the Foamscan analysis and additional reactor trials, a superficial gas velocity of  $1.9 \text{ mm s}^{-1}$  in combination with a protein concentration of  $1.75 \text{ g L}^{-1}$  was chosen. These settings were a compromise between sufficient foam stability in the foam-bed photobioreactor while still allowing for reasonable foam break-up. With these settings, the foam half-life is expected to be between 0.5 and 1.5 hours and the foam liquid holdup approximately 5.1 to 6.4% (Figure 3 A and B) when neglecting the effect of gas flow rates (as those did not had a significant effect above  $1.8 \text{ mm s}^{-1}$ ). The bubble size is expected to be between 0.27 and 0.42 mm (Figure 3 C).

The empty bed gas residence time is a good measure for the relative gas flow supplied to a foam-bed reactor and it allows for the comparison of different studies and reactors. The empty bed gas residence time is obtained by dividing the volume of the reactor by the volumetric gas flow rate entering the reactor. The empty bed gas residence time was 3.58 minutes, which is significantly longer than reported before for other foam-bed reactors (i.e. less than one minute) [16, 18-20, 32]. Our long residence time reflects reduced gassing, which may contribute to reduced operation costs when considering scale-up.

### 3.1.2 Designing foam break-up

In order to ensure efficient foam break-up in the foam-bed photobioreactor, various methods were experimentally tested for their suitability. These methods included bubble break-up due to natural destabilisation, foam centrifugation, mechanical disruption by a stirrer, and foam collapse due to physical contact with hydrophobic solid materials. First a brief overview of the approaches that were found not suitable for the foam-bed photobioreactor are listed. Natural foam destabilisation is a combined result of coalescence, coarsening and drainage. This method resulted in a dry, inhomogeneous foam, instead of the desired foam destabilisation with foam collapsing from the topmost layer only. A visible protein shell

remained at the maximum foam height in the reactor, originating from the proteins that were released from the bubbles' rigid stabilising films when the bubbles burst [45-47]. This effect led to protein depletion from the bulk and, consequently, the foam became less stable in time.

When using a continuous centrifuge, the foam was broken down efficiently. However, at the lowest required rotational speed for foam break-up, the microalgae also settled and accumulated in the centrifuge. A mechanical stirrer created a foam with smaller bubbles instead of collapsing the foam.

A hydrophobic sieve plate made of PDMS, described in a previous study [34], was also tested in two different configurations. When the foam entered from the bottom, the foam continuously rose in the foam breaker until reaching the plate. Some bubbles were not broken and consequently passed through the sieve, leading to liquid accumulation on the top of the sieve because liquid drainage was obstructed by the up-flowing gas. The latter problem was eliminated by passing the foam through the foam breaker from the top to the bottom. In this configuration the gas flow direction, and the natural drainage direction (due to gravitational force) corresponded, thus the liquid could easily pass through the sieve, although still some unbroken bubbles were left behind.

In order to further increase the foam break-up efficiency, the sieve was replaced by a packed bed column containing hydrophobic beads. The defoaming properties of solid hydrophobic particles are well studied and it appears that particles with high contact angles are particularly efficient in destabilising foams [48]. Two different bead materials were used together within the packed bed column: PDMS and PTFE beads. Furthermore, a hydrophobic coating was applied on the glass column (Sigmacote, Sigma). The contact angles of these materials in air

with water were reported to be 100° [49], 109° [50] for PDMS, 116° for PTFE [51], and 91° for glass coated with Sigmacote [52]. Other potential advantages of this packed bed column design are: 1) that the foam breaking efficiency of the packed column may be increased compared to that of the sieve due to the increased contact time and area between the material and the foam; 2) that the beads applied are large enough to not mix into the liquid phase; and 3) that relatively large beads, i.e. a large pore size, can be used thereby reducing the pressure drop in the reactor. According to our knowledge, this is the first study where a solid defoaming material was used for continuous defoaming in a foam-bed reactor system.

The beads were more efficient in foam breaking compared to the sieve plate according to experiments with the foam-bed photobioreactor. The efficiency of the foam breaker was dependent on the gas flow rates and surfactant concentrations. At low surfactant concentration and reduced gas flow rates, thus low foam loads, the foam breaker worked efficiently.

However, when the foam load was elevated, a foamy fluid instead of pure liquid was pumped back to the reactor. This did not seem to cause problems and a stable foam-bed could be maintained. A slight overpressure developed in the reactor due to the foam breaker, as it reduced the cross sectional area and created a resistance to the flow of the foam (approximately 4 % of the cross sectional area of the reactor remained open for foam flow in between the beads inside the foam breaker). The overpressure in the reactor was always under 60 mbar.

### **3.2 Microalgal growth in foam-bed photobioreactor**

*Chlorella sorokiniana* cells were cultivated for 8 hours in the foam-bed photobioreactor. The average growth rate in the foam-bed photobioreactor during these 8 hours was 0.10 h<sup>-1</sup>. This finding was based on the increase in cell volume concentration (Figure 4), which

corresponded with the measurements of optical density and cell number. These results indicate that microalgae can grow in liquid foams and that the photobioreactor developed is suitable for microalgae cultivation.

The growth rate achieved in the foam-bed reactor is good and comparable to other studies but lower than the maximal specific growth rate of *Chlorella sorokiniana* reported, which is  $0.27 \text{ h}^{-1}$  [53, 54]. The difference between the maximal growth rate and the growth rate reached in the foam-bed photobioreactor is related to the fact that not the whole microalgal culture is illuminated and that the average light intensity in the culture is below the saturation point, predominantly because of microalgal self-shading. More specifically, in the bulk liquid, foam breaker, and associated tubing, the cells were not receiving light to support their growth. Assuming an average of 5 % liquid holdup in the foam, approximately 30 % of the culture volume was not illuminated. In addition, the light intensity used was lower than in the studies where the maximum growth rate was reached [53, 54]. Moreover, biomass density was considerable resulting in microalgal self-shading.

In order to relate the achieved biomass densities to other studies, the growth was expressed as increase in dry weight concentration, for which a conversion factor of 0.5 was used to convert mL cell volume (Figure 4) to gram dry weight [55]. The biomass density on average increased from  $2.1$  to  $4.7 \text{ g L}^{-1}$  after 8 hours of growth. As a comparison, in experiments of microalgal suspension cultures the biomass density generally is  $1$  to  $3 \text{ g L}^{-1}$  at an equivalent specific growth rate ( $0.1 \text{ h}^{-1}$ ) and in reactors of comparable thickness [36, 56-58]. In these studies higher light intensities were applied than in the present study, indicating that the foam-bed photobioreactor allows for elevated biomass density cultures.

The finding that the growth rate of *Chlorella sorokiniana* in a foam-bed is in the same range as in comparable suspension cultivations demonstrates that *C. sorokiniana* cultures are able to withstand the shear stresses associated to foam bubble formation and collapse. This finding is supported by the stable and high maximum quantum yield of PSII photochemistry of the microalgal culture throughout the entire experiment. This is because it is known from other studies that shear stress during bubble formation at the sparger and bubble collapse in the headspace might damage microalgal cells [59-61], while it was also reported that the quantum yield of PSII photochemistry decreases during excessive shear stress acting on the cells [62]. At the start of the growth experiment, microalgae were acclimated to optimal growth conditions, as shown by a high quantum yield of 0.72–0.78. This was the quantum yield observed in a conventional flat panel photobioreactor, which served as inoculum for the foam-bed photobioreactor. During the 8 hours growth experiments the quantum yield did not change (Figure 4B), indicating that the integrity of the photosynthetic machinery of *C. sorokiniana* was conceivably not affected by foam bubble formation and break-up.

Quantification of growth in a foam-bed photobioreactor can easily be compromised. Hence, the following measures and measurements were done to exclude erroneous conclusions. First, the total cell volume concentration was determined by only taking into account cell diameters between 2 and 6  $\mu\text{m}$ , thus the reported values reflect only the microalgal biomass concentration and exclude any bacterial biomass. Second, the average ratio between microalgae concentration in the foam to their concentration in the bulk liquid was found to be  $0.9 \pm 0.2$ , indicating that the microalgae had equal distribution over the two phases. Thus, the measurements on the bulk liquid are representative for the whole reactor including the foam section. Finally, the humidity and temperature of the inlet and outlet gas of the reactor were continuously monitored in order to quantify liquid loss due to evaporation. Approximately 1.7

g of water was entering the reactor as vapour via the inlet gas in 8 hours, while 1.6 to 2.1 g water left as vapour via the outlet gas. The results indicate that less than half a gram of water had been evaporated during the whole reactor run, which is negligible compared to the total amount of water present (150 mL). Thus, the possibility of the microalgae biomass concentration increasing due to evaporative loss of water can be excluded, confirming that the concentration increase observed was solely due to microalgal growth.

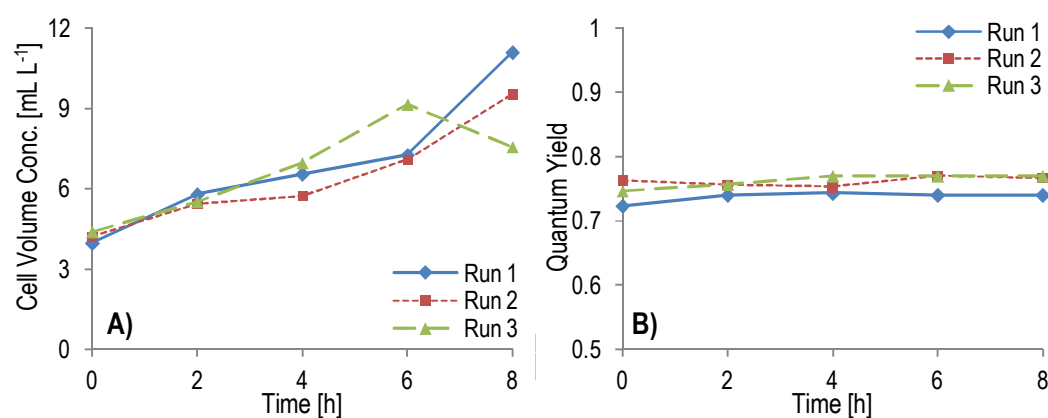


Figure 4: A) Microalgal growth in the foam-bed photobioreactor measured as microalgal cell volume concentration in time; B) Maximum quantum yield of PSII photochemistry ( $F_v/F_m$ ) during the three growth experiments.

### 3.3 Long-term stability of BSA –stabilized foam

The protein concentration in the cell free supernatant of reactor samples continuously decreased during the reactor runs (Figure 5). This was also confirmed by visual observations of decreasing foam stability. Larger gas bubbles appeared in time and the liquid content of the foam declined. This was also confirmed by a decreased recirculation flow, implying a decrease in the amount of foam leaving the reactor and/or a decreased liquid holdup of the foam.



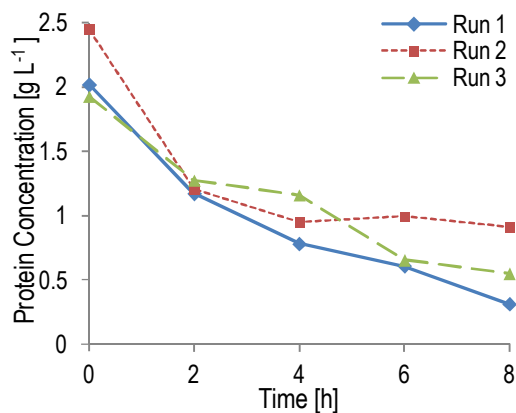


Figure 5: Protein concentration in the cell-free supernatant of the bulk liquid during three different 8 hour growth experiments in the foam-bed photobioreactor.

BSA molecules have a clear preference for the foam phase, indicated by the protein analysis of both the foam phase and the bulk liquid phase. While the bulk liquid phase protein concentration is decreasing below  $1 \text{ g L}^{-1}$  after 8 hours, the protein concentration in the foam only shows a small decline in time in comparison to its initial value of  $\sim 2.1 \text{ g L}^{-1}$  (data not shown). The observation of protein enrichment in the foam phase is in agreement with other studies [63].

The decreasing protein concentration in the bulk liquid could be due to protein aggregation because of foaming induced damage in the BSA molecules. Protein molecules experience conformational changes when foamed and, consequently, their properties and structure are altered as well, causing aggregation [42]. The aggregated protein might have been removed with the centrifugation step prior to the protein assay. Besides, several other reasons might stand behind the decline in protein concentration, including biodegradation by microorganisms present in the cultures [64], thermal degradation [65], or adsorption [66].

To test the alternative hypotheses on the origin of the decreasing protein concentration in the bioreactor experiments, additional experiments were done. Shake flasks containing BSA were inoculated with *C. sorokiniana* cultures and were placed in a dark incubator at 37°C. The protein and microalgal cell volume concentration were continuously monitored. The results of these shake flask experiments showed that neither the algae concentration neither the BSA concentration changed during the 9 days of experiments. This revealed that BSA did not adsorb to microalgal cells in a significant extent, as the cells were removed prior to the protein measurement. Furthermore, the possibility of consumption of the protein by *C. sorokiniana* or by the bacterial consortium present in the cultures can be excluded. These experiments also exclude the possibility of thermal degradation of BSA as the protein concentration remained unchanged while incubated at 37 °C. The possibility of BSA adsorption in the foam breaker was also tested. A protein solution of 2 g L<sup>-1</sup> BSA was flushed through the foam breaker device including the hydrophobic PTFE and PDMS beads. The results showed that the protein concentration remains unchanged, indicating that no adsorption took place to the foam breaker device and its content.

To summarize, we think it is most likely that the decrease of foam stability in time is due to protein denaturation due to foaming. Next to this, possibly the biodegradation of the protein by bacteria also contributed to the protein decrease in the reactor, since a few bacterial cells were observed in the reactor samples by microscopic analysis. The decrease in foam stability implies that BSA is not suitable for applications where continuous re-foaming of the surfactants is required. Therefore, BSA does not meet the requirements for long-term application within foam-bed photobioreactors, revealing the need for novel surfactants. Nevertheless, BSA is a good foaming agent in order to study foam-based microalgal growth on a time scale of multiple hours.

## 4. Conclusions

The results of this study suggest that the novel foam-bed photobioreactor can be a good alternative to conventional microalgae cultivation system. A foam-bed photobioreactor was successfully developed for microalgae cultivation and its ability to support microalgal growth has been confirmed. Aiming at optimal reactor performance, foam formation and foam break-up systems are essential. BSA protein was successfully used as foam stabilising. For efficient separation of the gas and liquid phase in the foam leaving the reactor a packed bed column filled with hydrophobic beads was developed. *Chlorella sorokiniana* showed an average specific growth rate of  $0.10 \text{ h}^{-1}$  in the foam-bed photobioreactor in combination with high PSII efficiency. The biggest limitation of the foam-bed photobioreactor was the short operational time of 8 hours due to protein depletion from the bulk liquid. For long-term operation of a foam-bed photobioreactor, a more stable foaming agent is required.

## 5. Acknowledgements

This project has received funding from the European Union's Seventh Framework Programme for research, technological development and demonstration under grant agreement no 613588.

## References

- [1] R.J. Shields, I. Lupatsch, Algae for aquaculture and animal feeds, *J. Anim. Sci.* 21 (2012) 23-37.
- [2] C. Posten, C. Walter, *Microalgal biotechnology: Integration and economy*, De Gruyter, Berlin, Boston 2012.
- [3] R.B. Draaisma, R.H. Wijffels, P.M. Slegers, L.B. Brentner, A. Roy, M.J. Barbosa, Food commodities from microalgae, *Curr. Opin. Biotechnol.* 24 (2013) 169-177.
- [4] R.H. Wijffels, M.J. Barbosa, M.H. Eppink, Microalgae for the production of bulk chemicals and biofuels, *Biofuels, Bioprod. Biorefin.* 4 (2010) 287-295.
- [5] J. Milledge, Commercial application of microalgae other than as biofuels: a brief review, *Rev. Environ. Sci. Biotechnol.* 10 (2011) 31-41.
- [6] R.N. Singh, S. Sharma, Development of suitable photobioreactor for algae production – A review, *Renewable Sustainable Energy Rev.* 16 (2012) 2347-2353.
- [7] F.G. Acien, J.M. Fernández, J.J. Magán, E. Molina, Production cost of a real microalgae production plant and strategies to reduce it, *Biotechnol. Adv.* 30 (2012) 1344-1353.
- [8] C.U. Ugwu, H. Aoyagi, H. Uchiyama, Photobioreactors for mass cultivation of algae, *Bioresour. Technol.* 99 (2008) 4021-4028.
- [9] N. Uduman, Y. Qi, M.K. Danquah, G.M. Forde, A. Hoadley, Dewatering of microalgal cultures: a major bottleneck to algae-based fuels, *J. Renewable Sustainable Energy* 2 (2010) 012701.
- [10] C. Posten, Design principles of photo-bioreactors for cultivation of microalgae, *Eng. Life Sci.* 9 (2009) 165-177.
- [11] M. Janssen, P.P. Lamers, M. de Haan, R.H. Wijffels, Growing microalgae or cyanobacteria in liquid-based foam, International patent application No. PCT/EP2013/073065, publication number WO 2014072294 A1, filed Nov. 5 2013, issued May 15, 2014, Wageningen.
- [12] A.A. Gaikwad, A.N. Bhaskarwar, Absorption of pure carbon-dioxide gas in a foam-bed reactor, *Proceedings of European Congress of Chemical Engineering (ECCE-6) Copenhagen, 2007.*
- [13] S.R. Asolekar, P.K. Deshpande, R. Kumar, A model for a foam-bed slurry reactor, *AIChE J.* 34 (1988) 150-154.
- [14] A.N. Bhaskarwar, D. Desai, R. Kumar, General model of a foam bed reactor, *Chem. Eng. Sci.* 45 (1990) 1151-1159.
- [15] M.B. Ripley, A.B. Harrison, W.B. Betts, R.K. Dart, A.J. Wilson, Enhanced degradation of a model oil compound in soil using a liquid foam-microbe formulation, *Environ. Sci. Technol.* 34 (2000) 489-496.
- [16] E. Kan, M.A. Deshusses, Development of foamed emulsion bioreactor for air pollution control, *Biotechnol. Bioeng.* 84 (2003) 240-244.
- [17] E. Kan, M.A. Deshusses, Continuous operation of foamed emulsion bioreactors treating toluene vapors, *Biotechnol. Bioeng.* 92 (2005) 364-371.
- [18] J. Song, Y. Kim, Y. Son, J. Khim, A bioactive foam reactor for the removal of volatile organic compounds: system performance and model development, *Bioprocess. Biosyst. Eng.* 30 (2007) 439-446.
- [19] F.G. Shahna, F. Golbabaee, J. Hamed, H. Mahjub, H.R. Darabi, S.J. Shahtaheri, Treatment of Benzene, Toluene and Xylene Contaminated Air in a Bioactive Foam Emulsion Reactor, *Chin. J. Chem. Eng.* 18 (2010) 113-121.
- [20] F.G. Shahna, F. Golbabaee, J. Hamed, H. Mahjub, H.R. Darabi, S.J. Shahtaheri, A bioactive foamed emulsion reactor for the treatment of benzene-contaminated air stream, *Bioprocess. Biosyst. Eng.* 33 (2010) 219-226.
- [21] N.S. Deshpande, M. Barigou, Performance characteristics of novel mechanical foam breakers in a stirred tank reactor, *J. Chem. Technol. Biotechnol. Biotechnology* 74 (1999) 979-987.
- [22] Y. Chisti, Animal-cell damage in sparged bioreactors, *Trends Biotechnol.* 18 (2000) 420-432.
- [23] A.C. Martinez, E. Rio, G. Delon, A. Saint-Jalmes, D. Langevin, B.P. Binks, On the origin of the remarkable stability of aqueous foams stabilised by nanoparticles: link with microscopic surface properties, *Soft Matter* 4 (2008) 1531-1535.
- [24] K. Miyamoto, O. Wable, J. Benemann, Vertical tubular reactor for microalgae cultivation, *Biotechnol. Lett.* 10 (1988) 703-708.
- [25] A.A. Gaikwad, N. Challapalli, A.N. Bhaskarwar, Carbonation of Barium Sulfide in a Foam-Bed Reactor, *Chem. Eng. Commun.* 197 (2010) 804-829.
- [26] A. Varshney, P. Agrawal, A.N. Bhaskarwar, Gas absorption with zero-order chemical reaction in a foam-bed reactor, *Chem. Eng. Sci.* 58 (2003) 3413-3424.
- [27] G.S. Reddy, A.N. Bhaskarwar, Modeling of Gas Absorption with a Zero-order Chemical Reaction in a Foam-bed Reactor: Comparison with Oxidation of Sodium Dithionite, *Chem. Eng. Sci.* 58 (2003) 3413-3424
- [28] M. Barigou, Foam rupture by mechanical and vibrational methods, *Chem. Eng. Technol.* 24 (2001) 659-663.
- [29] S. Takesono, M. Onodera, A. Ito, M. Yoshida, K. Yamagiwa, A. Ohkawa, Mechanical control of foaming in stirred-tank reactors, *J. Chem. Technol. Biotechnol.* 76 (2001) 355-362.
- [30] William H. Echols, Apparatus for breaking up a foam, U.S. Patent 3,298,615, filed Sept. 25 1964 and issued Jan. 17 1967, Fort Foote Village,
- [31] S. Takesono, M. Onodera, M. Yoshida, K. Yamagiwa, A. Ohkawa, Performance characteristics of mechanical foam-breakers fitted to a stirred-tank reactor, *J. Chem. Technol. Biotechnol.* 78 (2003) 48-55.
- [32] E. Kan, M.A. Deshusses, Cometabolic degradation of TCE vapors in a foamed emulsion bioreactor, *Environ. Sci. Technol.* 40 (2006) 1022-1028.
- [33] D.O. Hitzman, E.H. Wegner, Methanol foam fermentation to single cell protein by *Pseudomonas methanica*, U.S. Patent RE30,543, filed Jan 21, 1977, issued March 10 1981, Bartlesville, Okla.

- [34] M. Ishida, R. Haga, N. Nishimura, H. Matuzaki, R. Nakano, High cell density suspension culture of mammalian anchorage independent cells: Oxygen transfer by gas sparging and defoaming with a hydrophobic net, *Cytotechnology* 4 (1990) 215-225.
- [35] Y.-P. Wang, K. Yuan, Q.-L. Li, L.-P. Wang, S.-J. Gu, X.-W. Pei, Preparation and characterization of poly (N-isopropylacrylamide) films on a modified glass surface via surface initiated redox polymerization, *Mater. Lett.* 59 (2005) 1736-1740.
- [36] A.M. Kliphuis, L. de Winter, C. Vejraska, D.E. Martens, M. Janssen, R.H. Wijffels, Photosynthetic efficiency of *Chlorella sorokiniana* in a turbulently mixed short light-path photobioreactor, *Biotechnol. Progr.* 26 (2010) 687-696.
- [37] T. de Mooij, M. Janssen, O. Cerezo-Chinarro, J.H. Mussnug, O. Kruse, M. Ballottari, R. Bassi, S. Bujaldon, F.-A. Wollman, R.H. Wijffels, Antenna size reduction as a strategy to increase biomass productivity: a great potential not yet realized, *J. Appl. Phycol.* 27 (2014) 1063-1077.
- [38] N.R. Baker, Chlorophyll fluorescence: a probe of photosynthesis in vivo, *Annu. Rev. Plant Biol.* 59 (2008) 89-113.
- [39] F.J. Lech, M.B. Meinders, P.A. Wierenga, H. Gruppen, Comparing foam and interfacial properties of similarly charged protein-surfactant mixtures, *Colloids Surf., A* 473 (2015) 18-23.
- [40] P. Asharani, Y.L. Wu, Z. Gong, S. Valiyaveetil, Toxicity of silver nanoparticles in zebrafish models, *Nanotechnology* 19 (2008) 255102.
- [41] P. Wilde, A. Mackie, F. Husband, P. Gunning, V. Morris, Proteins and emulsifiers at liquid interfaces, *Adv. Colloid Interface Sci.* 108 (2004) 63-71.
- [42] J. Clarkson, Z. Cui, R. Darton, Protein denaturation in foam: II. Surface activity and conformational change, *J. Colloid Interface Sci.* 215 (1999) 333-338.
- [43] P. Stevenson, Hydrodynamic theory of rising foam, *Miner. Eng.* 20 (2007) 282-289.
- [44] S. Boonyasuwat, S. Chavadej, P. Malakul, J.F. Scamehorn, Surfactant recovery from water using a multistage foam fractionator: Part I effects of air flow rate, foam height, feed flow rate and number of stages, *Sep. Sci. Technol.* 40 (2005) 1835-1853.
- [45] J.F. Zayas, Foaming properties of proteins, in: J.F. Zayas, *Functionality of proteins in food*, Springer, Berlin, Heidelberg, 1997, pp. 260-309.
- [46] A. Saint-Jalmes, M.L. Peugeot, H. Ferraz, D. Langevin, Differences between protein and surfactant foams: Microscopic properties, stability and coarsening, *Colloids Surf., A* 263 (2005) 219-225.
- [47] M.A. Bos, T. van Vliet, Interfacial rheological properties of adsorbed protein layers and surfactants: a review, *Adv. Colloid Interface Sci.* 91 (2001) 437-471.
- [48] R. Pugh, Foaming, foam films, antifoaming and defoaming, *Adv. Colloid Interface Sci.* 64 (1996) 67-142.
- [49] J. Bongaerts, K. Fourtouni, J. Stokes, Soft-tribology: lubrication in a compliant PDMS-PDMS contact, *Tribol. Int.* 40 (2007) 1531-1542.
- [50] S. Bhattacharya, A. Datta, J.M. Berg, S. Gangopadhyay, Studies on surface wettability of poly (dimethyl) siloxane (PDMS) and glass under oxygen-plasma treatment and correlation with bond strength, *J. Microelectromech. Syst.* 14 (2005) 590-597.
- [51] T. Zawodzinski, S. Gottesfeld, S. Shoichet, T. McCarthy, The contact angle between water and the surface of perfluorosulphonic acid membranes, *J. Appl. Electrochem.* 23 (1993) 86-88.
- [52] S.N. Krylov, N.J. Dovichi, Single-cell analysis using capillary electrophoresis: influence of surface support properties on cell injection into the capillary, *Electrophoresis* 21 (2000) 767-773.
- [53] M. Janssen, T.C. Kuijpers, B. Veldhoen, M.B. Ternbach, J. Tramper, L.R. Mur, R.H. Wijffels, Specific growth rate of *Chlamydomonas reinhardtii* and *Chlorella sorokiniana* under medium duration light/dark cycles: 13-87 s, *J. Biotechnol.* 70 (1999) 323-333.
- [54] J. Van Wageningen, S.L. Holdt, D. De Francisci, B. Valverde-Pérez, B.G. Plósz, I. Angelidaki, Microplate-based method for high-throughput screening of microalgae growth potential, *Bioresour. Technol.* 169 (2014) 566-572.
- [55] M. Janssen, R. Wijffels, U. von Stockar, Biocalorimetric monitoring of photoautotrophic batch cultures, *Thermochim. Acta* 458 (2007) 54-64.
- [56] M. Cuaresma, M. Janssen, C. Vilchez, R.H. Wijffels, Horizontal or vertical photobioreactors? How to improve microalgae photosynthetic efficiency, *Bioresour. Technol.* 102 (2011) 5129-5137.
- [57] M.C. Franco, M.F. Buffing, M. Janssen, C.V. Lobato, R.H. Wijffels, Performance of *Chlorella sorokiniana* under simulated extreme winter conditions, *J. Appl. Phycol.* 24 (2012) 693-699.
- [58] M. Cuaresma, M. Janssen, C. Vilchez, R.H. Wijffels, Productivity of *Chlorella sorokiniana* in a short light-path (SLP) panel photobioreactor under high irradiance, *Biotechnol. Bioeng.* 104 (2009) 352-359.
- [59] J.M.S. Rocha, J.E.C. Garcia, M.H.F. Henriques, Growth aspects of the marine microalga *Nannochloropsis gaditana*, *Biomol. Eng.* 20 (2003) 237-242.
- [60] W. Hu, R. Gladue, J. Hansen, C. Wojnar, J.J. Chalmers, The Sensitivity of the Dinoflagellate *Cryptocodinium cohnii* to Transient Hydrodynamic Forces and Cell-Bubble Interactions, *Biotechnol. Progr.* 23 (2007) 1355-1362.
- [61] T.M. Sobczuk, F.G. Camacho, E.M. Grima, Y. Chisti, Effects of agitation on the microalgae *Phaeodactylum tricorutum* and *Porphyridium cruentum*, *Bioprocess. Biosyst. Eng.* 28 (2006) 243-250.
- [62] M. Leupold, S. Hindersin, G. Gust, M. Kerner, D. Hanelt, Influence of mixing and shear stress on *Chlorella vulgaris*, *Scenedesmus obliquus*, and *Chlamydomonas reinhardtii*, *J. Appl. Phycol.* 25 (2013) 485-495.
- [63] R.W. Schnepf, E.L. Gaden, Foam fractionation of proteins: concentration of aqueous solutions of bovine serum albumin, *J. Biochem. Microbiol. Tech. Eng.* 1 (1959) 1-11.
- [64] K. Watanabe, N. Takihana, H. Aoyagi, S. Hanada, Y. Watanabe, N. Ohmura, H. Saiki, H. Tanaka, Symbiotic association in *Chlorella* culture, *FEMS Microbiol. Ecol.* 51 (2005) 187-196.
- [65] I. Hayakawa, J. Kajihara, K. Morikawa, M. Oda, Y. Fujio, Denaturation of bovine serum albumin (BSA) and ovalbumin by high pressure, heat and chemicals, *J. Food Sci.* 57 (1992) 288-292.
- [66] H.B. Bull, Adsorption of bovine serum albumin on glass, *BBA* 19 (1956) 464-471.